Field-line mapping correlation of HHFW-induced divertor heating to power coupled into the SOL in front of the NSTX antenna*

R. J. Perkins[1], J.-W. Ahn[2], R. E. Bell[1], A. Diallo[1], S. Gerhardt[1], T. K. Gray[2], D. L. Green[2], J. C. Hosea[1], E. F. Jaeger[2], M. A. Jaworski[1], G. J. Kramer[1], B. P. LeBlanc[1], R. Maingi[2], A. McLean[2], C. K. Phillips[1], L. Roquemore[1], P. M. Ryan[2], S. Sabbagh[3], F. Scotti[1], G. Taylor[1], J. R. Wilson[1] and the NSTX Team

1 *Princeton Plasma Physics Laboratory, Princeton, NJ, USA*

2 *Oak Ridge National Laboratory, Oak Ridge, TN, USA*

3 *Columbia University, New York, NY,*

Introduction

High-harmonic fast-wave (HHFW) heating and current-drive efficiencies on NSTX can be significantly lowered by interactions of the HHFW with the edge plasma in the scrape-off layer (SOL) [1-5]. These edge interactions result in RF power deposition from the antenna to both the lower and upper divertor regions where bright spirals are produced, as shown in Fig. 1. The location of the spirals in the divertor regions is consistent with the hypothesis that HHFW power flows through the SOL to the divertor regions along magnetic field lines that pass in front of the antenna [6]. This includes the field lines across the SOL between the antenna and the last closed flux surface (LCFS), indicating that the HHFW power flow to the divertor regions occurs across the width of the SOL. This paper presents comparisons of measurements of power deposition effects in the divertor regions to SOL field strike patterns for magnetic field lines passing through the SOL midplane in front of the antenna. The agreement obtained between divertor infrared (IR) and optical camera data (locations shown in Fig. 1) supports the hypothesis that the HHFW power is flowing along SOL field lines and gives an indication of the RF power deposition radial profile across the SOL. These results are important for benchmarking advanced RF codes for predicting the amount of fast-wave power coupled to the SOL [7].

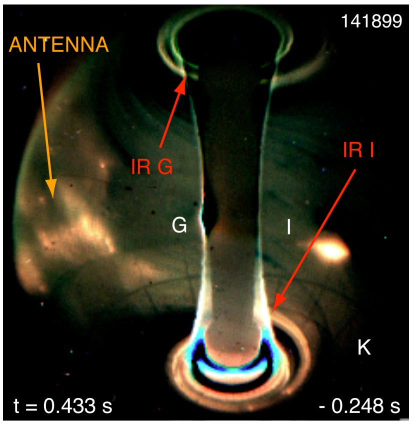

Figure 1. Camera view of "hot" RF produced spiral for shot 141899 with a magnetic pitch of ~ 40°. Conditions are D_2, B_T = 4.5 kG, I_P = 1 MA, P_{RF} = 1.4 MW, Ant k_f = $-8m^{-1}$, P_{NB} = 2 MW, H-mode with $n_e(0) \sim 5 \times 10^{19}$ m^{-3}, antenna-LCFS gap ~ 6.7 cm. Locations for antenna, ports B G I K, and IR camera views are noted.

Mapping of magnetic field lines from the SOL midplane in front of the antenna

If the HHFW power flows primarily along field lines in the SOL, tracing the field lines from the vicinity of the antenna to the divertor regions shows the path of the HHFW power.

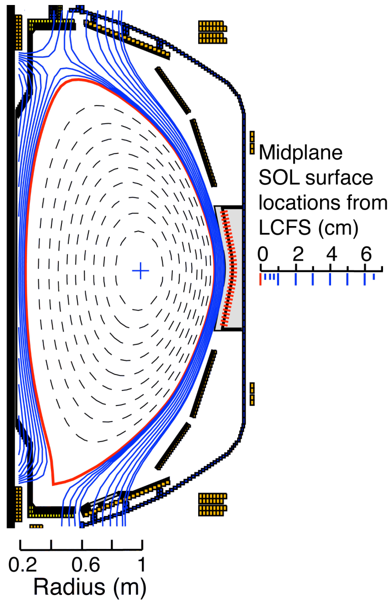

Figure 2. LRDFIT flux surfaces for mapping field lines from the midplane in front of the antenna to the divertor regions in the outer SOL for shot 141899 at t =0.435 sec. At midplane, the LCFS radius = 1.508 m and the antenna radius = 1.575 m.

In particular, the location at which HHFW power is deposited in the divertor regions is where the field lines strike the divertor. The LRDFIT04 [8] equilibrium reconstruction for the discharge of Fig. 1 is shown in Fig. 2 for t = 0.435 s. We use the full-orbit code SPIRAL [9] to follow field lines along flux surfaces from the SOL midplane in front of the antenna to the divertor regions. The particle trajectories can be taken as proxies for the field lines because the particles are launched with small velocities parallel to the field (1 eV deuterons) to minimize drifts. Figure 3 shows an ensemble of such strike points on the lower divertor. The field lines start at different SOL radii at the midplane, from 1.575 m (the major radius of the Faraday screen), down to 1.508 m (the midplane radius of the LCFS). The field lines also have a ninety degree toroidal spread to reflect the toroidal extent of the antenna. The collection of strike points form a spiral pattern on both the upper and lower divertors, matching the spiral RF heat depostion pattern observed in camera images (e.g. Fig. 1). Note that magnetic field lines emanating closest to the antenna strike the divertor region floor at the largest major radius and at a toroidal angle closest to the clockwise (viewed from above) end of the antenna. As the SOL midplane radius decreases toward the LCFS, the lines strike the floor at ever smaller major radius and at ever larger toroidal angle. Thus to the extent that the RF power flows to the divertor floor along field lines, the radial and toroidal deposition on the divertor floor indicates the power lost across the SOL in front of the antenna.

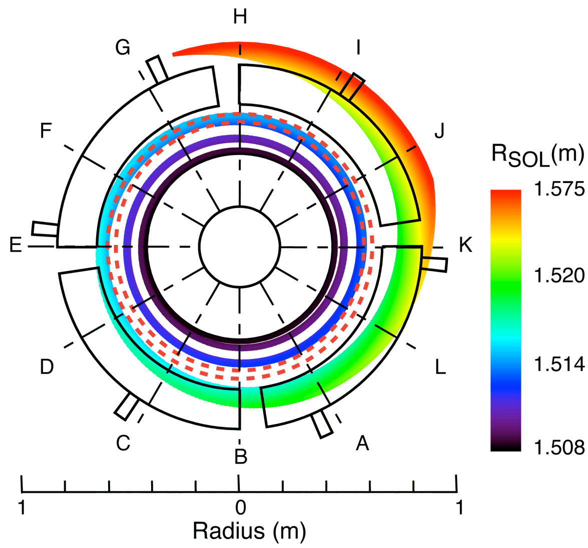

Figure 3. Magnetic field line strike points on lower divertor region for field lines originating between the antenna and the LCFS in the SOL at the midplane of the antenna for shot 141899 at t = 0.435 sec. (LRDFIT04 and conditions for Figs.1 and 2.)

Comparison of field strike points to measurements of RF heat deposition

There is good agreement between the field-line mapping and optical camera images taken of the divertor floor. Figure 4 is a LI I-filtered image from shot 141899 at t = 0.433 s [10].

The strike points computed with SPIRAL with EFIT02 [11] are overlaid on the image: the green points denote the strike points of field lines starting from the right-hand side of the antenna (as viewed in Fig.1), whereas the blue points represent lines from the left-hand side of the antenna. The first and second passes of the bright spiral fit nicely between these two sets of points, indicating that the HHFW power flow is largely aligned along field lines. At smaller radii, the field-line mapping does not agree as well with the physical spiral; we suspect that the equilibrium reconstruction for this shot might not be sufficiently accurate close to the LCFS.

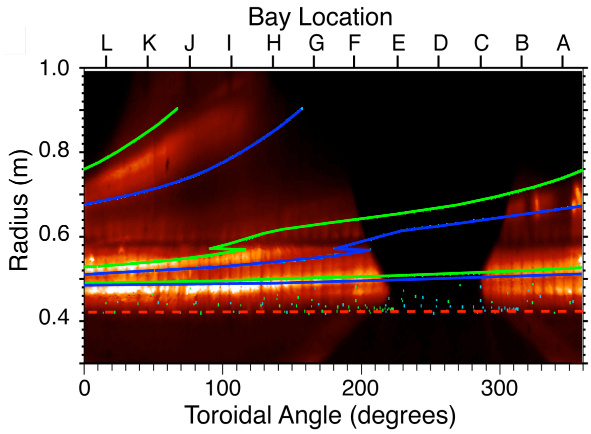

Figure 4. Comparison of the hot spiral location radially and toroidally viewed with LiI emission on the divertor floor with the location boundaries of the magnetic field strike points for EFIT02. (Conditions of Fig. 1 – shot 141899.)

The RF heat deposition to the divertor regions is best measured with the IR cameras located at Bay I for the lower divertor and at Bay G for the upper divertor [12]. Figure 5 shows an approximately radial profile of the heat deposited on the lower divertor during the RF heating, ΔQ, obtained by subtracting the heat profiles taken during (t = 0.444 s) and just before (0.244 s) the RF pulse. Beneath the heat profile are the strike points as computed by SPIRAL at Bay I. The RF-induced heat peaks generally coincide well with the strike points at Bay I, especially if heat conduction away from the peak deposition and the uncertainties of the EFIT reconstructions are taken into account. Note that the dip in the heat deposited around 60 cm is due to the CHI gap in the vessel. Also, the negative dip at the inner radius reflects the fact that the outer strike point is gradually moving outwards over the course of the discharge. The peak at R ≈ 0.91 m maps to an R_{SOL} ≈ 1.568 cm or 0.7 cm away from the face of the antenna. The peaks close to the outer strike zone correspond to lines emanating from very close to the LCFS, ~ 0.34 cm and 0.24 cm from the LCFS, respectively.

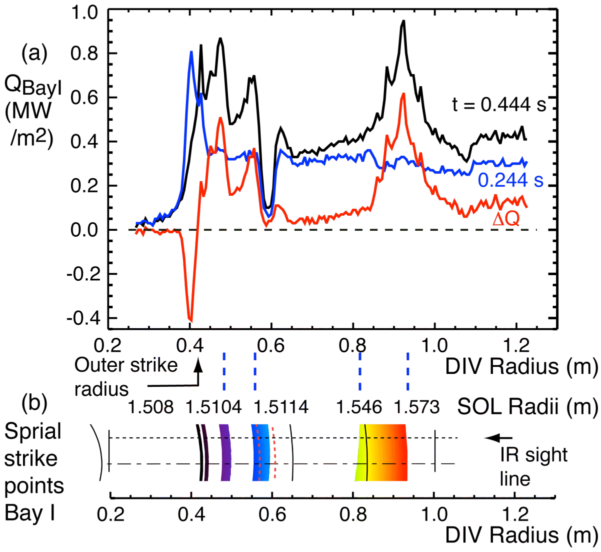

Figure 5. (a) IR heat flux to bottom divertor region at Bay I along sight line shown in (b). (b) Spiral strike points at Bay I. CHI gap is indicated with dashed red lines. (Conditions of Fig. 1.)

Figure 6 is an analogous plot for the upper divertor. Again here the locations of the peaks of the RF heat flux, ΔQ, agree well with the field line strike point mapping. However, the peaks are not as strong as for the lower divertor. This difference is likely due to up/down asymmetries in the RF heat flux and to the fact that the Bay G camera is not catching the most intense portion of the upper spiral. In particular, note that the field lines for the inner Bay I peaks do not reach the upper divertor region but go over the top of the plasma and strike the lower part of the center column (Fig. 2).

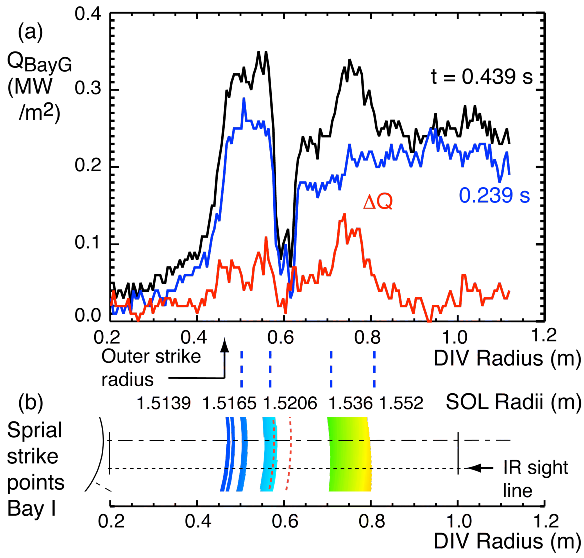

Figure 6. (a) IR power flux to upper divertor region at Bay G along sight line shown in (b). (b) Spiral strike points at Bay G. CHI gap is indicated with dashed red lines. (Conditions of Fig.1.)

Conclusions

In conclusion, the strike points computed with SPIRAL agree well with the position of the RF-induced spirals in both upper and lower divertors as measured with optical and IR cameras. Figures 4 and 5 combined suggest that RF heat deposition peaks near but in front of the antenna and very near the LCFS (the lithium light is brighter in these regions as is the light in Fig. 1). This result could be due to radial fast wave standing waves in the SOL and should be matched when benchmarking advanced RF codes that incorporate Poynting and kinetic power flows in the SOL to the divertor regions.

References

1. J.C. Hosea *et al.*, *Physics of Plasmas* **15** (2008) 056104.
2. C.K. Phillips *et al.*, *Nuclear Fusion* **49** (2009) 075015.
3. J.C. Hosea *et al.*, *AIP Conf Proceedings* **1187** (2009) 105.
4. G. Taylor *et al.*, *Physics of Plasmas* **17** (2010) 056114.
5. J.C. Hosea *et al.*, *AIP Conf Proceedings* **1406** (2011) 333.
6. R.J. Perkins *et al.*, to be published in *Physical Review Letters*.
7. D.L. Green *et al., Physical Review Letters* **107** (2011) 145001.
8. J. Menard, private communication.
9. G.J. Kramer *et al., 22 IAEA Fusion Energy Conference* (Geneva, 2008) CD-ROM file IT/P6-3.
10. F. Scotti *et al.*, submitted to *Rev. Sci. Instrum.* (2012)
11. S. Sabbagh *et al., Nuclear Fusion* **41** (2001) 1601.
12. D. Mastrovito *et al.*, *Review of Scientific Instruments* **74** (2003) 5090.

* *This work conducted under Contract Number DE-AC02-09CH11466 with the U.S. Department of Energy.*